In situ electron spin resonance of initial oxidation processes of Si surfaces

Takahide Umeda [a,b,*,1], Satoshi Yamasaki [a], Masayasu Nishizawa [a], Tetsuji Yasuda [a], Kazunobu Tanaka [a,b]

[a] *Joint Research Center for Atom Technology (JRCAT), National Institute for Advanced Interdisciplinary Research (NAIR), 1-1-4 Higashi, Tsukuba, 305-8562, Japan*
[b] *University of Tsukuba, Tsukuba, 305-8513, Japan*

Abstract

We have made for the first time electron spin resonance (ESR) measurements on Si(111)7 × 7 and Si(100)2 × 1 surfaces during the initial oxidation processes at room temperature. The present results clearly show that, at a very initial stage of oxidation of Si surfaces where only a few surface layers were oxidized, a variety of defects are formed that have not been seen in ex situ ESR studies of SiO_2/Si structures. © 2000 Elsevier Science B.V. All rights reserved.

1. Introduction

Electron spin resonance (ESR) detects defects and radicals with unpaired electrons such as dangling bonds (DBs) or hydrogen atoms. It is one of the best tools to reveal the microscopic and electronic structures of the point defects in semiconductors and insulators. This technique has been applied to investigate defects at the hetero-interface between Si and SiO_2, which is the most important structural part of silicon microelectronic devices. The nature of this interface is particularly important due to the decreasing thickness of the SiO_2 layer in future devices. Previous studies have found that: (i) the SiO_2/Si interfaces generate three sorts of Si DBs, so-called P_b [1,2], P_{b0} and P_{b1} [3–6]; (ii) such DBs are the origin of interface electrical traps and thus seriously degrade a device quality [7–10].

However, all previous ESR works were made on SiO_2/Si structures with an oxide layer over 0.5-nm thick. Recently, we have developed a novel ESR setup that enables ESR observations on clean Si surfaces. This setup allows us to explore the defect formation on the Si surfaces during exposure of oxygen gas. This paper describes results of our ESR observation on Si(111)7 × 7 and Si(100)2 × 1 surfaces when the oxide layers grew from 0 (i.e., the clean surface) to around 0.5 nm in thickness.

---

* Corresponding author. Tel.: +81-298-54-2634; fax: +81-298-54-2642.
E-mail address: umeda@jrcat.or.jp (T. Umeda).
[1] Research fellow of the Japan Society for the Promotion of Science.

2. Experimental: UHV–ESR system

To observe the oxidation of clean and well-defined Si surfaces, it is necessary to prepare ultrahigh-vacuum (UHV) environments inside a cylindrical space (1 cm diameter × 1 cm height) for ESR measurements. Thus, we developed a novel UHV–ESR system, which is shown in Fig. 1. In the gap of the ESR magnet, a microwave cavity was combined with a high-purity vitreous silica tube of a small UHV chamber with a base pressure of 1×10^{-8} Pa. Two Si wafers (double-sided mirror finish, $8 \times 0.3 \times 0.03$ cm in dimensions) with a 0.05-cm separation between the two were supported on the tip of a transfer rod and were transferred from end-to-end in the chamber. Both ends of the rectangular wafers were attached to electrical contacts to allow direct current heating.

We used Si(111) and Si(100) wafers with a very high resistivity (over 1000 Ω cm) to reduce the microwave losses. The wafers were subjected to the conventional RCA cleaning and to a pre-heating at 600–700°C under UHV. Finally, they were cleaned by flash heating with direct current at 1000–1100°C for about 30 s. During the flash heating, the chamber pressure was maintained at about 10^{-7} Pa. The surface was oxidized at room temperature by exposure to pure molecular oxygen without any hot filaments. After flash heating and oxidation, the surface structures were confirmed by reflection high energy electron diffraction (RHEED), and then the surfaces were subjected to the ESR measurements.

The ESR spectra were measured by a BRUKER ELEXSYS X-band spectrometer at room temperature with a microwave frequency of 9.6 GHz, power of 1–200 mW and a magnetic field modulation of 0.4–1.0 mT at 100 kHz. The spectrometer parameters for each spectrum were adjusted within the above range to get the highest signal-to-noise ratio and to prevent an artificial distortion of the spectrum. The number of defects observed here was between 1×10^{12} and 2×10^{13} within an ESR-active area of 1.2 cm^2, which is close to the detection limit of our ESR instrument (approximately 10^{11} spins/mT). Hence, it was necessary to accumulate each ESR spectrum for 6–12 h, and for 1 day in the longest cases. During the accumulation, the chamber was evacuated to the base pressure, which prevents the surfaces being changed by contaminants. We observed ESR spectra for different orientation angles, θ, between the wafer axes (either [111] or [100]) and the magnetic field ($\boldsymbol{B}$) direction.

3. Oxidation of Si(111)7 × 7 surface

Fig. 2(a) shows the ESR spectra of Si(111) wafers just before flash heating, when $\theta = 0°$ ($\boldsymbol{B}//[111]$) and 90° ($\boldsymbol{B}//[\bar{1}10]$). These spectra show the ESR signal of the P_b center [1,2], whose principal g values are estimated to be $g_{//} = 2.002$ and $g_{\perp} = 2.009$ for $\theta = 0°$ and 90°, respectively. Since the origin of the P_b center has been identified as a [111]-oriented Si DB at the $SiO_2/Si(111)$ interface [1,2], it is reasonable to observe the P_b center in our sample with an oxide layer formed by the RCA treatment. In addition to the P_b, this sample showed a small ESR signal, which is tentatively attributed to the 19° P_{b0} centers [6]. The 19° P_{b0} centers are essentially identical to the P_{b0} observed in $SiO_2/Si(100)$ interfaces and they are positioned towards [$1\bar{1}1$], [$\bar{1}11$], and [$11\bar{1}$]. As is our case, these centers were observed as a minority in $SiO_2/Si(111)$ structures [6]. In the figure, the resonant positions of the P_b and 19° P_{b0} (vertical dashed lines) are calculated by referring to the previous g data [1,2,6]. Naturally, the P_b signal observed here showed a good agreement with the calculation, and the 19° P_{b0} case is likely to be consistent, too.

After the wafers were cleaned by the flash heating, the P_b and 19° P_{b0} signals disappeared, as shown in Fig. 2(b), simply because the oxide layer was
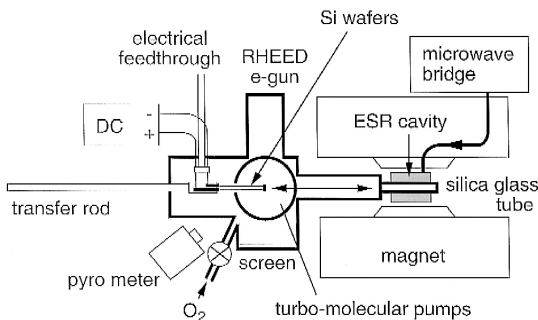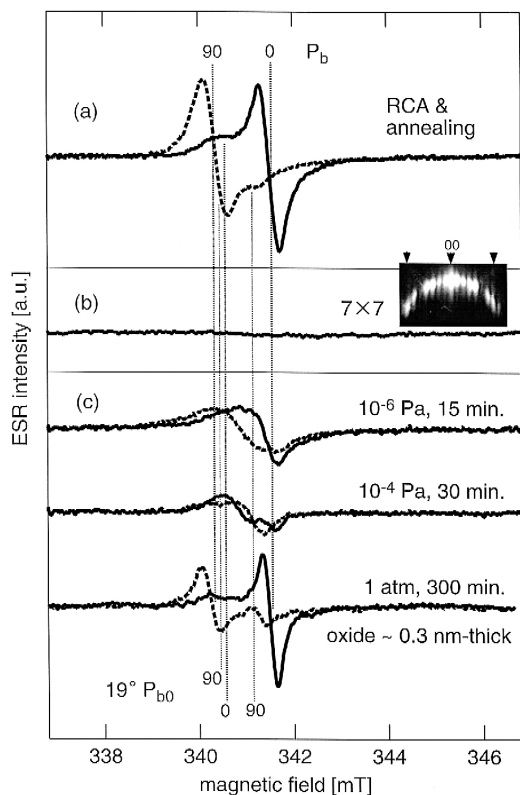

Fig. 1. Schematic view of UHV–ESR system.

Fig. 2. ESR observation of Si(111) wafers during room temperature oxidation processes. ESR spectra (a) before flash heating, (b) for 7×7 surface after flashing and its RHEED pattern in the 0th Laue zone (arrows indicate fundamental reflections), and (c) during oxidation processes. Solid and broken lines were obtained for $\theta = 0°$ ($B // [111]$) and $90°$ ($B // [\bar{1}10]$), respectively. Vertical dashed lines indicate the resonant positions of P_b and $19° P_{b0}$ for $\theta = 0°$ and $90°$ and their thickness represents a relative intensity of each signal.

evaporated completely. RHEED measurements reveal a clear 7×7 reconstructed structure on this surface (Fig. 2(b)). Therefore, we expected to see an ESR signal due to the large number ($\geq 10^{13}$ cm^{-2}) of surface DBs on the 7×7 surface [11,12]. However, room temperature ESR measurements could not reveal any DB signals. It is speculated that we did not see the surface DBs is due to the broadening of the ESR line, which causes a large loss of signal intensity. This issue will be discussed in a forthcoming paper.

Although the clean surface showed no appreciable ESR signals, the exposure of the surface to oxygen

molecules caused drastic changes in the ESR spectrum. Fig. 2(c) shows the evolution of ESR spectra as a pressure of oxygen was increased from 10^{-6} Pa to 1 atm. After the exposure to 1 atm oxygen, the P_b signal appears again, simply because the oxide layer was formed again on the surface. At that time, the oxide layer thickness was measured to be around 1 bilayer (approximately 0.3 nm) by ex situ Auger electron spectroscopy (AES). The $19° P_{b0}$ signal also seems to appear again, although its intensity is less than in the spectrum (a).

On the other hand, before the 1-bilayer-thick oxidation was completed, various transient ESR spectra with an appreciable θ-dependence were observed, as is seen in Fig. 2(c), that are obviously different from the P_b spectra observed either before flashing or after the 1-bilayer-thick oxidation. Furthermore, in the 10^{-4}-Pa oxidation, the transient ESR spectrum involves two or more signals. Judging from the simulated resonant positions (vertical dashed lines), these new transient signals are not due to $19° P_{b0}$. We have also confirmed that the P_{b1} center is not consistent with the transient signals. Therefore, it is suggested that surroundings of the transient defects and/or their microscopic and electronic structures are different from those of the P_b-type defects. We emphasize that they are seen transiently only during the period for the 1-bilayer-thick oxidation and disappear afterwards; eventually, we can only see the P_b-type defects. Thus, the transient defects have not been detected previous ESR studies of SiO_2/Si structures.

We also note that our results shown here are quite different from previous results of Haneman et al. [13–16] who observed Si surface states by ESR. They detected only an isotropic resonance of $g \sim 2.0055$ in their Si samples that is quite similar to a DB signal in amorphous Si [17].

4. Oxidation of Si(100)2 $\times$ 1 surface

We also made ESR studies of Si(100) surfaces during room temperature oxidation processes as summarized in Fig. 3. For the case of Si(100), the P_{b0} and P_{b1} centers were seen in the SiO_2/Si(100) interface of our initial sample (Fig. 3(a)), which is consistent with the previous ESR works [3–5]. After the flash heating, these interfacial defects vanished
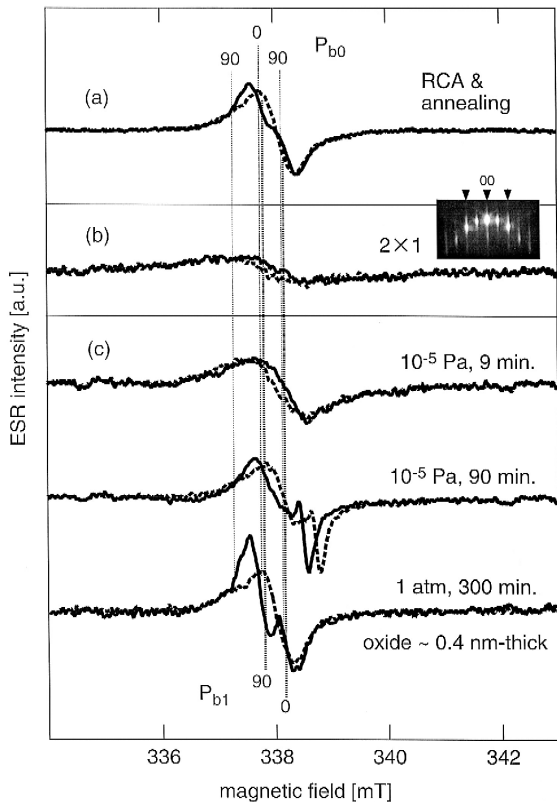
Fig. 3. ESR spectra of Si(100) wafers (a) before flash heating, (b) after flashing and a 2×1 RHEED pattern of the surface (cf. Fig. 2(b)), and (c) during room temperature oxidation processes, which were measured for $\theta = 0°$ ($\boldsymbol{B}//[100]$, solid lines) and $90°$ ($\boldsymbol{B}//[011]$, broken lines). We also indicate the resonant positions of P_{b0} and P_{b1} by vertical dashed lines, as is the same as Fig. 2.

completely due to the removal of the oxide. The new surface showed the 2×1 reconstruction in a RHEED pattern (Fig. 3(b)) and also a broad resonance in the ESR spectrum which corresponds to the spin density of an order of 10^{12} cm^{-2}. This resonance has the same positions as the P_{b1} center, and it was tentatively assigned to a Si DB at one end of a strained Si–Si dimer at the $SiO_2/Si(100)$ interface [4,5]. Therefore, the novel surface signal observed here may be related to defected dimers on the Si(100)2×1 surface. To be conclusive, we need more data such as a precise θ-dependence of this resonance.

As in the case of Si(111), the Si(100) surface was also greatly affected by oxygen exposure as shown in Fig. 3(c). Before the exposure to 1 atm oxygen, a variety of transient ESR spectra were observed which

have not been detected in previous ESR studies [3–5]. Those transient spectra showed significant angular dependence and a complex overlap of two or more signals. We also found that the transient defects exhibit different resonant positions with respect to the P_{b0} and P_{b1} (see vertical dashed lines in Fig. 3).

When an oxide layer was getting thicker up to 1 bilayer (approximately 0.4 nm in thickness measured by ex situ AES and consistent with a photoemission data [18]) by 1 atm oxygen exposure, the transient signals disappeared, and instead, the P_{b0} and P_{b1} signals dominated again. Detailed analyses of the ESR spectra will be given in the future, which will give us a novel information on the microscopic mechanism of the oxidation involving the defect formation.

5. Conclusion

Using a novel UHV–ESR setup, we have observed in situ defect formation on Si(111)7×7 and Si(100)2×1 surfaces during room temperature oxidation. Our ESR measurements revealed a variety of defects not previously detected in ex situ ESR studies [1–10] at the initial stage of oxidation of Si surfaces.

Acknowledgements

References

[1] K.L. Brower, Appl. Phys. Lett. 43 (1983) 1111.
[2] W.E. Carlos, Appl. Phys. Lett. 50 (1987) 1450.
[3] E.H. Poindexter, P.J. Caplan, B.E. Deal, R.R. Razouk, J. Appl. Phys. 52 (1981) 879.
[4] A. Stesman, V.V. Afanas'ev, J. Appl. Phys. 83 (1998) 2449.
[5] A. Stesmans, B. Nouwen, V.V. Afanas'ev, Phys. Rev. B 58 (1998) 15801.

[6] A. Stesmans, Appl. Phys. Lett. 48 (1996) 973.

[7] P.J. Caplan, E.H. Poindexter, B.E. Deal, R.R. Razouk, J. Appl. Phys. 50 (1979) 5847.

[8] P.M. Lenahan, P.V. Dressendorfer, J. Appl. Phys. 55 (1984) 3495.

[9] E.H. Poindexter, G.J. Gerardi, M.-E. Rueckel, P.J. Caplan, N.M. Johnson, D.K. Biegelsen, J. Appl. Phys. 56 (1984) 2844.

[10] G.J. Gerardi, E.H. Poindexter, P.J. Caplan, N.M. Johnson, Appl. Phys. Lett. 49 (1986) 348.

[11] J.E. Demuth, B.N.J. Persson, A.J. Schell-Sorokin, Phys. Rev. Lett. 51 (1983) 2214.

[12] J. Ortega, F. Flores, A.L. Yeyati, Phys. Rev. B 58 (1998) 4584.

[13] D. Haneman, Jpn. J. Appl. Phys. Suppl. 2, Pt. 2 (1974) 371.

[14] M.F. Chung, D. Haneman, J. Appl. Phys. 37 (1966) 1879.

[15] D. Haneman, Phys. Rev. 170 (1968) 705.

[16] D. Haneman, M.F. Chung, A. Taloni, Phys. Rev. 170 (1968) 719.

[17] T. Umeda, S. Yamasaki, J. Isoya, K. Tanaka, Phys. Rev. B 59 (1999) 4849.

[18] M. Morita, T. Ohmi, E. Hasegawa, M. Kawakami, M. Ohwada, J. Appl. Phys. 68 (1990) 1272.